Geophys. J. Int. (1990) **102**, 445–453

Rheology of the lithosphere in the East African Rift System

K. Fadaie[1] and G. Ranalli[2]
[1]*Geophysics Division, Geological Survey of Canada, Ottawa* K1A 0Y3, *Canada*
[2]*Department of Earth Sciences and Ottawa-Carleton Geoscience Centre, Carleton University, Ottawa* K1S 5B6, *Canada*

Accepted 1990 February 20. Received 1990 February 19; in original form 1989 May 17

SUMMARY

The rheological properties of the lithosphere in the East African Rift System are estimated from regional heat flow and seismic constraints. Heat flow data are used to infer average, maximum, and minimum geotherms for the Eastern Rift, the Western Rift, and the surrounding shield (having surface heat flow of 106 ± 51, 68 ± 47, and $53 \pm 19\,\mathrm{mW\,m^{-2}}$, respectively). Combining the geotherms with brittle and ductile deformation laws for a lithosphere of appropriate structure and composition yields rheological profiles, thickness of brittle layers, and thickness and total strength of the lithosphere. The thickness of the uppermost brittle layer varies from 10 ± 2 km in the Eastern Rift, to 18^{+6}_{-5} km in the Western Rift, and 26+ km in the shield; seismicity is confined to the brittle layers. The rheological thickness of the lithosphere in Eastern Rift (23^{+8}_{-9} km), Western Rift, and shield is approximately in the the ratio 1:2.5:5, and matches the elastic flexural thickness. The total resistance to deformation is one order of magnitude larger in the shield than in the rifted regions ($\sim 10^{12}\,\mathrm{N\,m^{-1}}$), where the whole lithosphere is probably in a state of failure.

Key words: East African Rift, heat flow, rheology of the lithosphere.

1 INTRODUCTION

The East African Rift System (EARS), the longest continental rift in the world, splits into two branches just north of latitude 10°S. The eastern and western branches are separated by the Precambrian rocks of the Tanganyika shield (Fig. 1). Gravity and seismic studies provide evidence for a thinned lithosphere underlain by anomalous low-density material beneath the two branches of EARS, and a thick shield lithosphere in between (Fairhead 1976; Savage & Long 1985).

The purpose of this paper is to analyse the rheological properties of the lithosphere in EARS. To this end, heat flow data are used to infer approximate geotherms for the two branches of the rift and the surrounding region. The geotherms, together with seismic constraints on the structure and composition of the lithosphere, are combined with deformation laws to yield rheological profiles (strength envelopes). From rheological profiles we obtain depth to brittle–ductile transition, lithospheric thickness, and total lithospheric strength for each subregion. The results are compared with other kinds of geophysical evidence such as depth distribution of earthquakes and flexural thickness of the lithosphere.

2 REGIONAL HEAT FLOW

Heat flow measurements for the region between 5°N and 15°S latitude, and 25°E and 40°E longitude, have been compiled from the world data collection by Jessop, Hobart & Sclater (1976), reviews by Morgan (1982, 1984) and original sources (see below). The search has been facilitated by access to the heat flow database of the Swiss Federal Institute of Technology (ETH-Zurich). In the absence of reliability indicators, we have used all available data, grouping sites into a single item only where they are closely spaced (<10 km). We have followed usual practice and expressed the heat flow distribution for a given region by the mean and standard deviation of the available data.

Heat flow values in EARS are shown in Fig. 2. In the Western Rift (WR), measurements have been made in Lake Kivu (Degens *et al*. 1973), Lake Tanganyika (Degens, Von Herzen & Wong 1971), and Lake Malawi (Von Herzen & Vacquier 1967). The last is considered part of WR because of the continuity in structural trend (see Fig. 1) and similarity in average heat flow. Uncorrected means and standard deviations (with the number of items in parentheses) are $73 \pm 70\,\mathrm{mW\,m^{-2}}$ ($n = 5$) for Lake Kivu, $50 \pm 35\,\mathrm{mW\,m^{-2}}$ ($n = 12$) for Lake Tanganyika, and 22 ± 13

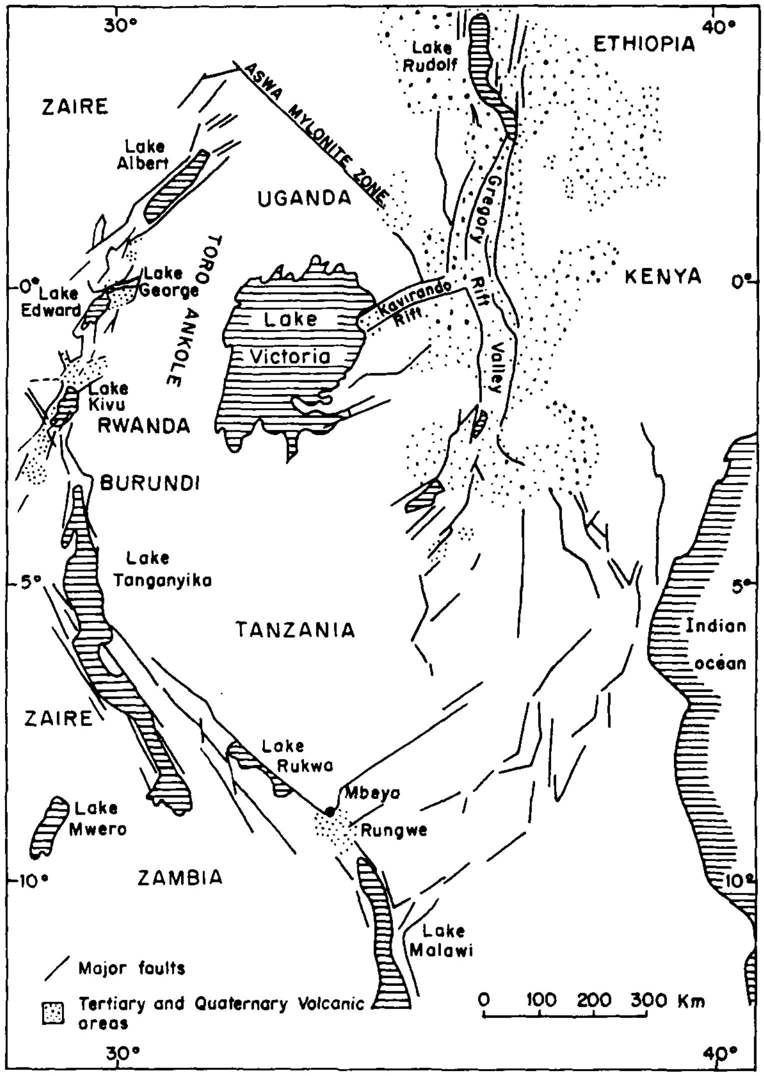

Figure 1. The East African Rift System (from King 1970).

($n = 12$), 96 ± 25 ($n = 5$), and $31 \pm 3\,\mathrm{mW\,m^{-2}}$ ($n = 3$) for the northern (north of 11.5°S), central, and southern (south of 12.5°S) parts of Lake Malawi, respectively.

Heat flow in the Eastern Rift (ER) has been measured on land both on the rift floor and on the shoulders and surrounding shield (Morgan 1973; Evans 1975; Williamson 1975; cf. summary in Morgan 1982). Uncorrected means and standard deviations are 106 ± 51 ($n = 13$), 61 ± 12 ($n = 5$), and $49 \pm 20\,\mathrm{mW\,m^{-2}}$ ($n = 13$) for the rift floor, western shoulder, and eastern shoulder, respectively. The combined shoulders value ($53 \pm 19\,\mathrm{mW\,m^{-2}}$) is not significantly different from the background value in eastern Africa ($58 \pm 16\,\mathrm{mW\,m^{-2}}$; Evans 1975).

The discrepancies between our compilation and that of Morgan (1982) are negligible, and probably due to minor differences in grouping and the fact that we have not rejected any 'anomalous' values. Data scatter is very high, possibly related to groundwater flow and Quaternary volcanic activity. The width of the high heat flow band in each branch, where controls exist, is narrow (<100 km) and coincides with the rift floor.

Heat flow measurements in WR, having been taken on lake bottoms, should be corrected, where applicable, for two effects: (i) bottom water warming where bottom water circulation is lacking, and (ii) sedimentary blanketing. The former applies to Lake Tanganyika and Lake Malawi (Degens *et al.* 1971); the latter to all three lakes unless sedimentation is nil.

It is useful to have at least a semi-quantitative idea of the magnitude of the corrections. The effect of bottom water warming on the temperature gradient can be approximated by using the analytical solution for a semi-infinite solid subject to a step change in surface temperature (Carslaw & Jaeger 1959). The gradient change is

$$\Delta\left(\frac{dT}{dz}\right)_{z=0} = \frac{T_1 - T_0}{[\pi\kappa(t - t')]^{1/2}} \tag{1}$$

where $T_1 - T_0$ is the change in surface temperature, occurring at $t = t'$, and κ is the thermal diffusivity. The effect of sedimentary blanketing on the temperature gradient can be estimated from the relation (Von Herzen,

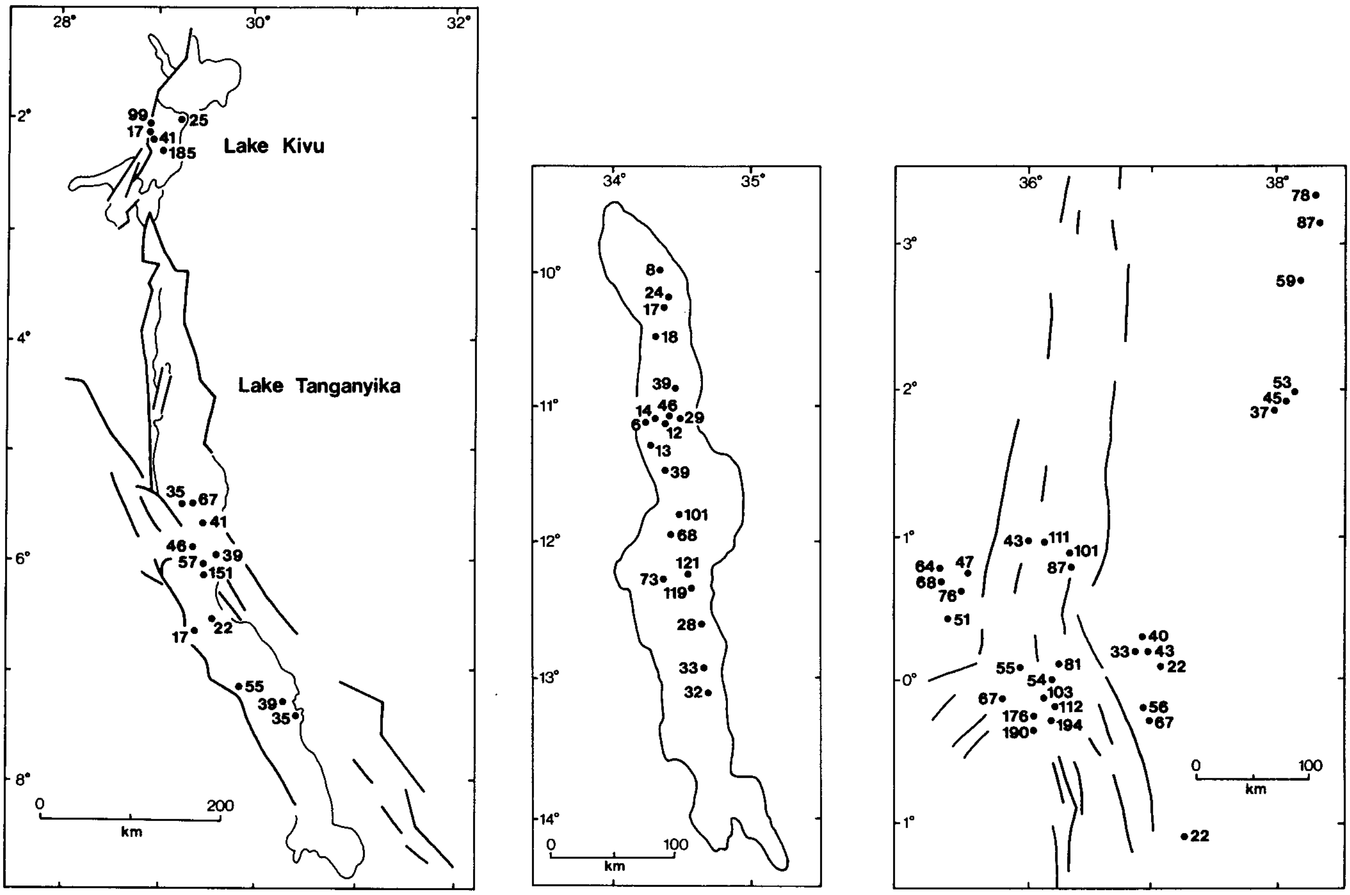

Figure 2. Heat flow in WR (left: lakes Kivu and Tanganyika; centre: Lake Malawi) and in ER (right).

Finckh & Hsu 1974)

$$\left(\frac{1}{\gamma}\frac{dT}{dz}\right)_{z=0} = (1+2\tau^2)\,\mathrm{erfc}\,(\tau) - \frac{2}{(\pi)^{1/2}}\,\tau\exp(-\tau^2) \qquad (2)$$

where γ is the corrected gradient, dT/dz the present (measured) gradient, and the dimensionless parameter $\tau = (U/2)(t^*/\kappa)^{1/2}$ is related to the sedimentation rate U and the time t^* since beginning of sedimentation.

Thermal diffusivity in lake sediments clusters around $0.4\times10^{-6}\,\mathrm{m^2\,s^{-1}}$ (Von Herzen & Vacquier 1967). Sedimentation rates have been estimated from ^{14}C measurements to be on the average 0.05, 0.35, and 0.25 cm $\mathrm{yr^{-1}}$ in Lake Tanganyika and the northern and central parts of Lake Malawi, respectively (Von Herzen & Vacquier 1967; Degens *et al.* 1971). The rate is effectively nil for the southern part of Lake Malawi, and we have assumed it to be 0.10 cm $\mathrm{yr^{-1}}$ in Lake Kivu, where it is unknown. Using these values and assuming $T_1 - T_0 = 10\,°\mathrm{C}$ since the end of the glacial period ($t - t' = 10^4$ yr), and $t^* = 10^5$ yr (corresponding to a sedimentary thickness of 200 m at an average rate of 0.2 cm $\mathrm{yr^{-1}}$), we obtain corrected heat flow values of $82\pm78\,\mathrm{mW\,m^{-2}}$ for Lake Kivu, $65\pm36\,\mathrm{mW\,m^{-2}}$ for Lake Tanganyika, and $67\pm46\,\mathrm{mW\,m^{-2}}$ for the whole of Lake Malawi. The uncertainty in the correction depends on the variability of the parameters in equations (1) and (2), and is less than ±25 per cent in most cases.

The overall average heat flow for WR, after corrections, is $68\pm47\,\mathrm{mW\,m^{-2}}$, that is, noticeably less than the value of $106\pm51\,\mathrm{mW\,m^{-2}}$ for ER. In a way, estimation of 'average' heat flow in this manner masks the large along-rift variability; in particular, there seems to be a correlation between high heat flow, transverse structural trends, and volcanicity (Fadaie 1987). The representative values, however, match well those observed in other continental rift systems (Morgan 1982), and confirm that 'wet' rifts (i.e., associated with profuse volcanism; Mohr 1982) have usually higher heat flow than rifts where volcanic activity is relatively minor.

3 REPRESENTATIVE GEOTHERMS

In order to calculate a rheological profile for a given region, a geotherm must be chosen. This is difficult to do in terms of surface heat flow only. Although seismic information on the structure of the lithosphere in EARS is available (see e.g. Nolet & Mueller 1982), data on the distribution of heat producing elements in the crust are lacking. We therefore calculate steady-state geotherms (the differences between steady-state and transient geotherms are not large, especially for high heat flow; see Pollack & Chapman 1977) for three different cases, based on analogies with other regions. First, we assume that heat generation decreases exponentially with depth (Lachenbruch 1970), and neglect the p, T-dependence of thermal conductivity. In such case, the geotherm is given by (see e.g. Lachenbruch & Sass 1978)

$$T(z) = \frac{1}{K}\{q_r z + b^2 A_0[1 - \exp(-z/b)]\}. \tag{3}$$

The chosen parameter values are K (thermal conductivity) $= 2.5\,\mathrm{W\,m^{-1}\,°C^{-1}}$, A_0 (surface heat production) $= 2.0\,\mu\mathrm{W\,m^{-3}}$, and b (characteristic depth) $= 10$ km. These values are central in their ranges (cf. review by Chapman 1986). As to the reduced heat flow q_r (that is, the flux coming from beneath the enriched uppermost crust), we assume in the first instance that all the variability in surface heat flow is contributed by the reduced heat flow (i.e. $q_r = q_0 - bA_0$, where q_0 is surface heat flow). In the second case, we take $q_r = 0.6q_0$ as proposed by Pollack & Chapman (1977), which implies that the variability in surface heat flow depends on both shallow and deep contributions. Finally, we use the model of Chapman (1986), in which the lithosphere is subdivided into layers, each with constant heat production. The temperature in the ith layer is

$$T_i(z) = T_{i-1} + \frac{q_{i-1}z}{K_i} - \frac{A_i z^2}{2K_i} \tag{4}$$

where T_{i-1} and q_{i-1} are temperature and heat low at the top of the layer, A_i and K_i are the relevant thermal parameters, and depth z is measured from the top of the layer. We consider a simple three-layer model with $A = 1.2$, 0.4, $0.02\,\mu\mathrm{W\,m^{-3}}$ and $K = 2.5$, 2.5, $3.0\,\mathrm{W\,m^{-1}\,°C^{-1}}$ in the upper crust, lower crust, and lithospheric upper mantle, respectively. Any more refined layering would be unwarranted, given our lack of detailed information on the chemistry and composition of the crust in EARS. The parameter values

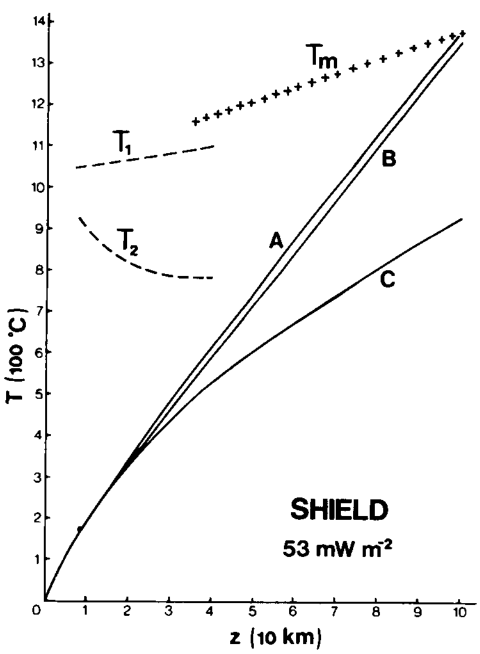

Figure 3. Geotherms for shield, ER, and WR (for surface heat flow as shown). A—geotherm calculated from equation (3) with $q_r = q_0 - bA_0$; B—geotherm calculated from equation (3) with $q_r = 0.6q_0$; C—geotherm calculated from equation (4). T_m is solidus for a slightly hydrated upper mantle; T_1, T_2 are dry and wet solidus for the lower crust.

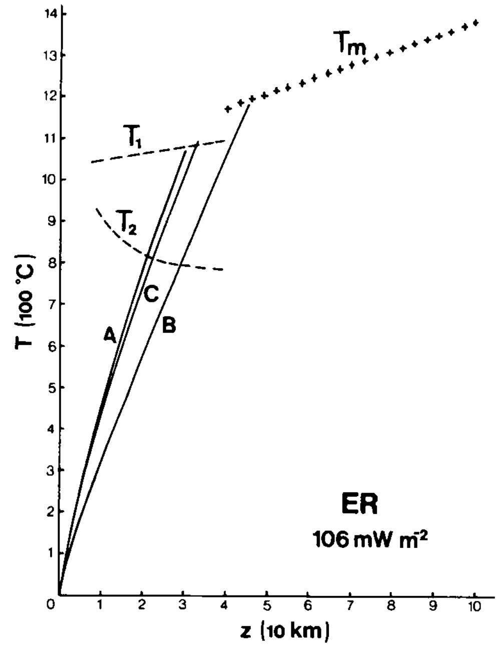

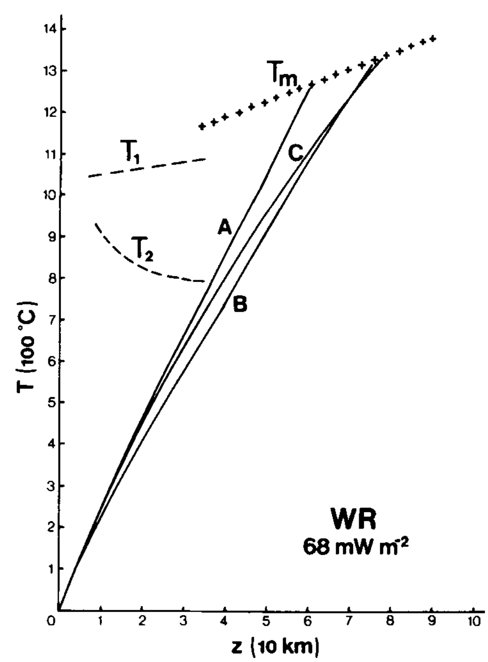

Figure 3. *(continued)*

are averages from compilations (Chapman 1986) and measurements in southern Africa (Nicolaysen, Hart & Gale 1981) and the Canadian shield (Ashwal *et al.* 1987).

The three geotherms calculated according to the above procedures are shown in Fig. 3 for three representative values of surface heat flow (53, 68, and $106\,\mathrm{mW\,m^{-2}}$). Differences are within ±50 °C in most of the lithosphere for ER and WR, but the 'cool' geotherms obtained for the shield from equation (3) are much higher than the corresponding one from (4). The former are clearly overestimates, as there is no basis for extrapolating equation (3) below crustal depths (Lachenbruch & Sass 1978). We use therefore the geotherms obtained from equation (4), with the relevant parameter values, in the estimation of rheological profiles.

The effects of variations in surface heat flow are shown in Fig. 4, where three geotherms are shown for each region (WR, ER, and surrounding shield), assuming an uncertainty of ±20 per cent in average heat flow. A representative upper mantle solidus (Pollack & Chapman 1977), together with 'dry' and 'wet' lower crustal solidus (Mysen 1981), is also shown. The spread in estimated temperature increases with decreasing surface heat flow. Correspondingly, uncertainties in rheological profiles will be larger for the shield region, and comparatively much less for the rift

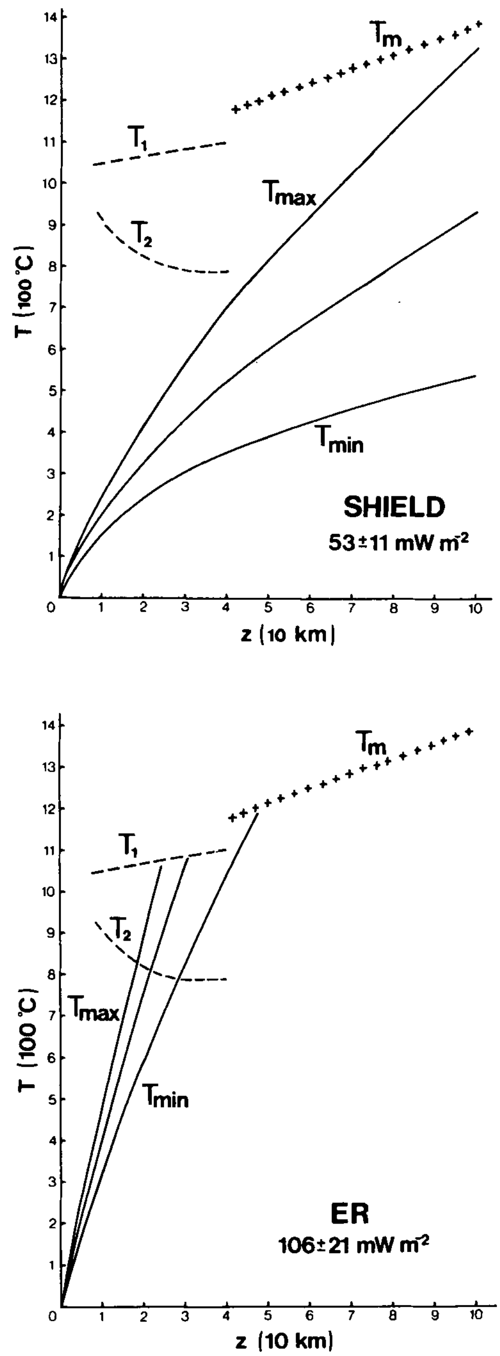

Figure 4. Average, maximum, and minimum geotherms estimated for shield, ER, and WR for surface heat flow values as shown.

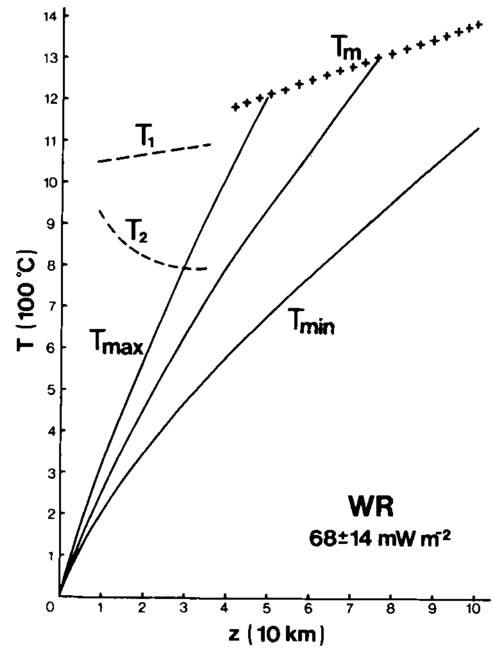

Figure 4. (*continued*)

regions. The effects of uncertainties in other thermal parameters seldom exceed ±10 per cent (Chapman 1986). Our calculated geotherms are intended to be representative of the average properties of each subregion, and do not reflect local conditions (e.g., variations along strike in the rift floors).

4 RHEOLOGICAL PROFILES

The two deformation laws for the construction of rheological profiles of the lithosphere are (see e.g. Ranalli 1987): (i) a frictional shear failure criterion which can be expressed as (Sibson 1974)

$$\sigma_1 - \sigma_3 = \beta \rho g z (1 - \lambda) \tag{5}$$

where $\sigma_1 - \sigma_3$ is the critical stress difference, β a parameter depending on the type of faulting, ρ the average density of the overlying material at depth z, g the acceleration due to gravity, and λ the pore fluid factor (ratio of water pressure to overburden pressure); and (ii) a ductile power-law creep equation based on the experimentally determined flow behaviour of silicate polycrystals at high temperature (cf. Carter & Tsenn 1987; Kirby & Kronenberg 1987; Ranalli 1987 for reviews)

$$\sigma_1 - \sigma_3 = \left(\frac{\dot{\epsilon}}{B}\right)^{1/n} \exp\left(\frac{E}{nRT}\right) \tag{6}$$

where $\dot{\epsilon}$ is strain rate, T absolute temperature, R the gas constant, and $B, n,$ and E material parameters that are either independent or only weakly dependent on temperature and pressure.

The occurrence of ductile rather than brittle deformation depends on the relative magnitude of the ductile creep strength and the brittle strength. If the critical stress difference for frictional failure is less than the creep strength, brittle faulting will occur; in the opposite case,

Table 1. Flow parameters used in the calculation of rheological profiles (from Carter & Tsenn 1987; Kirby & Kronenberg 1987).

Layer	Rock type	B ($MPa^{-n}s^{-1}$)	n	E($kJ\ mol^{-1}$)
Upper crust	Quartz diorite	1.3×10^{-3}	2.4	219
Lower crust	Diabase	3.2×10^{-3}	3.3	268
Mantle (dry)	Dunite (dry)	3.2×10^{4}	3.6	535
Mantle (wet)	Dunite (wet)	2.0×10^{3}	4.0	471

deformation will be by ductile flow. Calculation of a rheological profile, therefore, requires the choice of a geotherm and the estimation of parameters in equations (5) and (6). In equation (5), which is T-independent, we have taken $\beta = 0.75$, the appropriate value for normal faulting (Sibson 1974), $\lambda = 0.36$ (assuming the pore water pressure to be equal to the hydrostatic pressure), and rock densities derived from the seismic model of Nolet & Mueller (1982). The creep strength in equation (6) is estimated using a representative strain rate $\dot{\epsilon} = 10^{-15}\,s^{-1}$, the geotherms shown in Fig. 4, and values for the creep parameters (given in Table 1) matching the densities and seismic velocities of the seismic model. This gives and upper crust of intermediate (granodioritic to quartz–dioritic) composition (20 km thick in ER and surrounding shoulders, 14 km thick in WR), a lower crust of intermediate to basic (quartz–dioritic to basaltic) composition (with Moho at $z = 40$ km in ER and shoulders, $z = 35$ km in WR), and a peridotitic upper mantle.

Two sources of uncertainty are the precise composition of the various layers and the uncertainties in the creep parameters for a given rock type. To this one must add the effect of a change in strain rate (the creep strength varies by ~2 for a strain rate variation of one order of magnitude).

In the brittle field, equation (5) is valid for all relevant rock types, but the parameter β depends on the coefficient of friction. Our chosen value (for normal faulting) fits the data with minor scatter at confining pressures pertaining to the crust (Sibson 1974), but probably overestimates the strength of mantle brittle layers, if any. In the ductile field, the creep strengths of quartz- and plagioclase-rich rocks (from granodioritic to anorthositic and basaltic composition) differ by less than one order of magnitude under crustal conditions (Ranalli 1987), and therefore our models do not depend critically on minor changes in composition. The creep parameters chosen give creep strengths that are in the central range of those obtained experimentally for a given rock type (Carter & Tsenn 1987; Kirby & Kronenberg 1987). Their uncertainties are typically of the order of 10–20 per cent, but their combined effect depends on the sign of the individual variations. Assuming an uncertainty of ±10 per cent in E and ±20 per cent in n, we find that for both quartz diorite and dunite at 1000 K the most unfavourable combination of variations results in uncertainties of one order of magnitude in the creep strength, and usually much less.

Rheological profiles are shown in Fig. 5 for both 'dry' (i.e. having the rheology of dry dunite) and 'wet' (dunite with some H_2O content) upper mantle. Parameters of particular interests are the depth to the brittle–ductile transition, lithospheric thickness, and total strength.

The brittle–ductile transition in nature is transitional rather than sharp, but as the transition occurs over a range of only a few kilometres, a point estimation is a sufficiently good approximation at a lithospheric scale. Since the transition is defined as the depth at which brittle strength

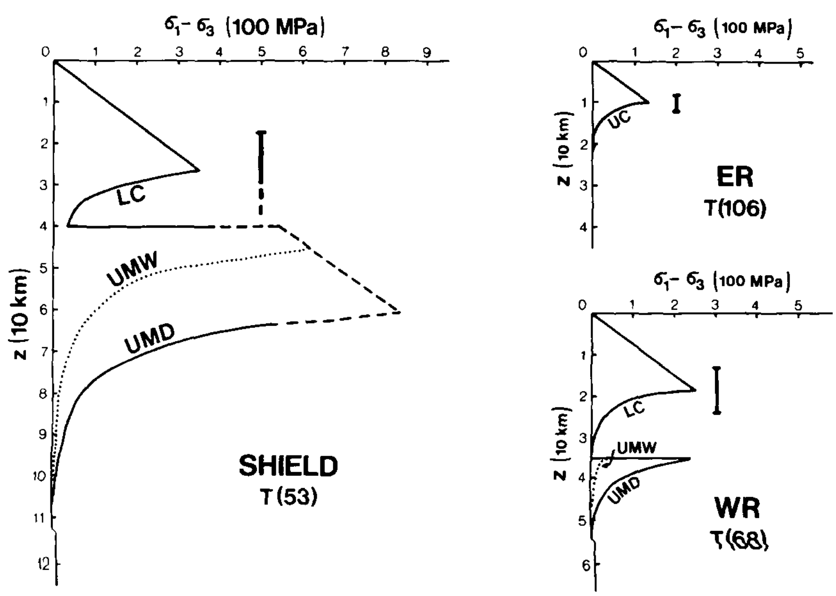

Figure 5. Rheological profiles for shield, ER, and WR for geotherms corresponding to average heat flow in each subregion. Brittle strength of the upper mantle, where applicable, is dashed to denote extrapolation from crustal shear failure criterion. UC, LC, UMW, and UMD denote creep strength for upper crust, lower crust, wet upper mantle, and dry upper mantle, respectively. Error bars indicate uncertainty in depth of the brittle–ductile transition as a function of surface heat flow, assuming that the limiting geotherms in each subregion are T_{max} and T_{min} as shown in the previous figure.

Table 2. Rheological characteristics of the lithosphere in EARS. [$T(q_0)$—geotherm for surface heat flow q_0 (mW m^{-2}); d—thickness of topmost brittle layer; L—rheological thickness of lithosphere; Σ—total force per unit width; σ_L—total strength. Central values are for average geotherm, limit values (in brackets) for maximum and minimum geotherm. 'Dry' and 'wet' refer to the upper mantle].

Subregion	Geotherm	d(km)	L(km)	Σ (N m^{-1})$^{(1)}$	σ_L(MPa)$^{(1)}$
Shield, dry	T(53±11)	26(17,130)$^{(2)}$	135(84,∞)$^{(4)}$	2.8x10^{13}	207
Shield, wet		26(17, 95)$^{(3)}$	121(75,∞)	1.5x10^{13}	124
ER$^{(5)}$	T(106±21)	10(8,12)	23(14,31)$^{(6)}$	0.9x10^{12}	39
WR, dry	T(68±14)	18(13,24)$^{(7)}$	65(48,102)	3.9x10^{12}	60
WR, wet			58(43,93)	2.9x10^{12}	50

Notes (see also discussion in the text):
(1) Values for average geotherm.
(2) For T(53), a sub-Moho brittle layer ($40 \le z \le 60$ km) is also present.
(3) For T(53), a sub-Moho brittle layer ($40 \le z \le 45$ km) is also present.
(4) ∞ denotes that no lower boundary of the lithosphere is encountered down to z = 150 km.
(5) No differences for wet or dry mantle.
(6) L_{max} neglects a thin sub-Moho layer (2 or 7 km thick for wet and dry mantle, respectively), where creep strength is larger than 1 MPa but within error limits (σ < 3 MPa).
(7) For T(54), a sub-Moho brittle layer is present (5 or 15 km thick for wet or dry mantle, respectively).

becomes equal to creep strength, it can be obtained directly by equating equations (5) and (6), expressing T as a function of z, and solving for depth (cf. also Ranalli 1987). We have estimated it for maximum, average, and minimum geotherms for each subregion, assuming a ±20 per cent uncertainty in surface heat flow, and the results are shown in Fig. 5 and Table 2. Uncertainties are very large in the case of the shield, but quite tolerable for ER and WR. For the colder geotherms, the uppermost mantle is also brittle.

The rheological thickness of the lithosphere can be defined as the depth at which some lower limit of strength is reached, and below which there are no further discontinuities in strength (to take into account the fact that often the lower crust is soft, but underlain by a strong upper mantle). A critical strength in the 1–10 MPa range agrees with usual estimations of upper mantle strength and minimizes the difference between rheological thickness and thermal thickness, defined as the depth to the $0.85T_m$ isotherm (Pollack & Chapman 1977; Ranalli 1990). The rheological thickness is calculated directly from equation (6) and a suitable geotherm. Results are shown in Table 2. Again, estimates for low surface heat flow have a larger uncertainty than those for higher heat flow.

Rheological profiles yield also the total lithospheric strength, defined as

$$\sigma_L = \frac{1}{L}\int_0^L (\sigma_1 - \sigma_3)(z)\,dz \tag{7}$$

where $(\sigma_1 - \sigma_3)(z)$ expresses the dependence of strength on depth, and L is the rheological thickness. The total strength (or the corresponding force per unit width, $\Sigma = \sigma_L L$) is a measure of the average stress (or force) required to extend the lithosphere at a given rate. Since what matters is the relative value of total strength in different tectonic regions, we have calculated it for the average heat flow in ER, WR, and surrounding shield; the qualitative uncertainty is probably of the order of ±25 per cent (a conservative estimate for ER and WR, but perhaps optimistic for the shield). Results for both dry and wet upper mantle are shown in Table 2. They are comparable to values obtained in regions of similar tectonic characteristics (see e.g. Kusznir & Park 1987; Lynch & Morgan 1987; Steckler & Ten Brink 1986; Ranalli 1990).

5 DISCUSSION

The basic point of this paper is that tolerably accurate rheological profiles (with semi-quantitative error limits) can be obtained from estimates of average heat flow and an approximate knowledge of the structure and composition of the lithosphere. The analysis leads to the prediction of certain observables (i.e. depth to brittle–ductile transition, thickness, and strength of the lithosphere) that can be compared with estimates obtained by different geophysical means.

Since interplate seismicity is mostly confined to brittle layers (see e.g. Meissner & Strehlau 1982; Sibson 1982; Chen & Molnar 1983), the distribution of seismicity with depth should provide a good check for the estimated depth of the brittle–ductile transition. Accurate focal depths (±4 km) of 11 earthquakes in EARS (four in ER and seven in WR) have been determined by Shudofski (1985). The only shock in ER with focal depth (28 km) below our estimate for the brittle–ductile transition is situated outside the rift. Two events in WR have hypocentres in the lower crust: of these one (focal depth 29 km) is situated outside the rift's bounding faults; the other (focal depth 23 km) is within the rift, but the uncertainty in hypocentre determination overlaps the uncertainty in the estimate of brittle layer thickness. If the lateral extent of weaker lithosphere coincides approximately with the width of the high heat flow band, therefore, no earthquakes in either WR or ER occur unequivocally in the ductile lower crust (see also the discussion by Shudofsky *et al.* 1987). There appears to be a tendency, however, for earthquakes to occur in the lower part of the brittle layer, where the stress in higher, a fact already noted by Meissner & Strehlau (1982). Both depth to brittle–ductile transition and distribution of earthquakes in ER are comparable to those in the eastern Basin-and-Range in the American Cordillera (Smith & Bruhn 1984).

In any case, the correlation between brittleness and seismicity is not absolute. Instabilities in ductile deformation may occur (Hobbs, Ord & Teyssier 1986), and earthquakes unequivocally situated in the lower crust have been occasionally detected (see e.g. Deichmann 1987). On the whole, however, the correlation between brittleness and seismicity provides a good first-order check on rheological profiles.

The effective elastic plate thickness beneath the East African Plateau has been determined by Ebinger *et al.* (1989) on the basis of analysis of gravity and topographic data. Stable cratonic areas have a thickness of 64–90 + km; the region encompassing both ER and WR and the Tanganyika shield has average thickness ~50 km; subregions including the rift valleys yield the smallest estimates (21–36 km). These values, although not allowing differentiation between ER and WR, and in rough agreement with our estimates of lithospheric thickness.

The total strength of the lithosphere has been modelled for various lithospheric structures and geotherms by Vink, Morgan & Zhao (1984) and Lynch & Morgan (1987), who predicted forces per unit width in the range $(0.7\text{–}3.2) \times 10^{12}\,\mathrm{N\,m^{-1}}$ for 'hot' (Basin-and-Range type) lithosphere, and $(1.5\text{–}6.0) \times 10^{13}\,\mathrm{N\,m^{-1}}$ for 'continental shield' lithosphere. The values in EARS are within these ranges. Since available estimates of tectonic force per unit width in the lithosphere cluster in the range $(1\text{–}5) \times 10^{12}\,\mathrm{N\,m^{-1}}$, with $10^{13}\,\mathrm{N\,m^{-1}}$ as an order-of-magnitude upper limit (see Carter & Tsenn 1987; Kusznir & Park 1987; and Ranalli 1987 for reviews), it is possible that the lithosphere in ER (and possibly also in WR) may be in a state of failure, as suggested also by flexural studies (Ebinger *et al.* 1989).

ACKNOWLEDGMENTS

We thank Drs J.-J. Wagner (University of Geneva) and D. Mayer-Rosa (Swiss Federal Institute of Technology, Zurich) for help in obtaining the heat flow data file. The comments of two reviewers were very useful. This work was supported by the Natural Sciences and Engineering Research Council of Canada through a grant to G. R. E. Lambton and L. Bender did the typing and drafting.

REFERENCES

Ashwal, L. D., Morgan, P., Kelley, S.A. & Percival, J. A., 1987. Heat production in an Archean crustal profile and implications for heat flow and mobilization of heat-producing elements, *Earth planet. Sci. Lett.*, **85**, 439–450.

Carslaw, H. S. & Jaeger, J. C., 1959. *Conduction of Heat in Solids*, 2nd edn, Clarendon Press, Oxford.

Carter, N. L. & Tsenn, M. C., 1987. Flow properties of continental lithosphere, *Tectonophysics*, **136**, 27–63.

Chapman, D. S., 1986. Thermal gradients in continental crust, in *The Nature of the Lower Continental Crust*, pp. 63–70, eds Dawson, J. B., Carswell, D. A., Hall, J. & Wedephol, K. H., Geol. soc. Lond. Sp. Publ., **24**.

Chen, W. P. & Molnar, P., 1983. Focal depths of intracontinental and intraplate earthquakes and their implications for the thermal and mechanical properties of the lithosphere, *J. geophys. Res.*, **88**, 4183–4214.

Degens, E. T., Von Herzen, R. P. & Wong, H. K., 1971. Lake Tanganyika: water chemistry, sediments, geological structure, *Naturwissensch.*, **58**, 229–241.

Degens, E. T., Von Herzen, R. P., Wong, H. K., Deuser, W. G. & Jannasch, H. W., 1973. Lake Kivu: structure, chemistry and biology of an East African rift lake, *Geol. Rundschau*, **62**, 245–277.

Deichmann, N., 1987. Focal depths of earthquakes in northern Switzerland, *Ann. Geophys.*, **5B**, 395–402.

Ebinger, C. J., Bechtel, T. D., Forsyth, D. W. & Bowin, C. O., 1989. Effective elastic plate thickness beneath the East African and Afar plateaus and dynamic compensation of the uplifts, *J. geophys. Res.*, **94**, 2883–2901.

Evans, T. R., 1975. Terrestrial heat flow in eastern Africa and the North Sea, *PhD thesis*, University of London.

Fadaie, K., 1987. Geophysical and isotopic constraints on the lithosphere in the East African Rift System, *PhD thesis*, Carleton University, Ottawa.

Fairhead, J., 1976. Structure of the lithosphere beneath the Eastern Rift, East Africa, deduced from gravity studies, *Tectonophysics*, **30**, 269–298.

Hobbs, B. E., Ord, A. & Teyssier, C., 1986. Earthquakes in the ductile regime, *Pure appl. Geophys.*, **124**, 309–336.

Jessop, A. M., Hobart, M. A. & Sclater, J. G., 1976. The world heat flow data collection—1975, *Geothermal Series*, vol. 5 Earth Physics Branch, Ottawa.

King, B. C., 1970. Volcanicity and rift tectonics in east Africa, in *African Magmatism and Tectonics*, pp. 263–283, eds Clifford, T. N. & Gass, I. G., Oliver & Boyd, Edinburgh.

Kirby, S. H. & Kronenberg, A. K., 1987. Rheology of the lithosphere: selected topics, *Rev. Geophys.*, **25**, 1219–1244.

Kusznir, N. J. & Park, R. G., 1987. The extensional strength of the continental lithosphere: its dependence on geothermal gradient, and crustal composition and thickness, in *Continental Extensional Tectonics*, pp. 35–52, eds Coward, M. P., Dewey, J. F. & Hancock, P. L., Geol. soc. Lond. Sp. Publ., **28**.

Lachenbruch, A. H., 1970. Crustal temperature and heat production: implications of the linear heat flow relation, *J. geophys. Res.*, **75**, 3291–3300.

Lachenbruch, A. H. & Sass, J. H., 1978. Models of an extending lithosphere and heat flow in the Basin and Range Province, *Geol. Soc. Am. Mem.*, **152**, 209–250.

Lynch, H. D. & Morgan, P., 1987. The tensile strength of the lithosphere and the localization of extension, in *Continental Extensional Tectonics*, pp. 53–65, eds Coward, M. P., Dewey, J. F. & Hancock, P. L., Geol. soc. Lond. Sp. Publ., **28**.

Meissner, R. & Strehlau, J., 1982. Limits of stresses in continental crust and their relationship to depth-frequency distribution of shallow earthquakes, *Tectonics*, **1**, 73–89.

Mohr, P., 1982. Musings on continental rifts, in *Continental and Oceanic Rifts*, pp. 293–309, ed. Palmason, G., Am. geophys. Union Geodyn. Series vol. 8, Washington, DC.

Morgan, P., 1973. Terrestrial heat flow studies in Cyprus and Kenya, *PhD thesis*, University of London.

Morgan, P., 1982. Heat flow in rift zones, in *Continental and Oceanic Rifts*, pp. 107–122, ed. Palmason, G., Am. geophys. Union Geodyn. Series vol. 8, Washington, DC.

Morgan, P., 1984. The thermal structure and thermal evolution of the continental lithosphere, in *Structure and Evolution of the Continental Lithosphere*, pp. 107–193, eds Pollack, H. N. & Rama Murthy, V., Pergamon Press, Oxford.

Mysen, B., 1981. Melting curves of rocks and viscosity of rock-forming melts, in *Physical Properties of Rocks and Minerals*, pp. 361–407, eds Touloukian, Y. S., Judd, W. R. & Roy, R. F., McGraw-Hill, New York.

Nicolaysen, L. O., Hart, R. J. & Gale, N. H., 1981. The Vredefort radioelement profile extended to supracrustal strata at Carletonville, with implications for continental heat flow, *J. geophys. Res.*, **86**, 10 653–10 661.

Nolet, G. & Mueller, S., 1982. A model for the deep structure of the East African rift system from simultaneous inversion of teleseismic data, *Tectonophysics*, **84**, 151–178.

Pollack, H. N. & Chapman, D. S., 1977. On the regional variation of heat flow, geotherms, and lithospheric thickness, *Tectonophysics*, **38**, 279–296.

Ranalli, G., 1987. *Rheology of the Earth*, Allen & Unwin, London.

Ranalli, G., 1990. Regional variations in lithosphere rheology from heat flow observations, in *Heat Flow and Structure of the Lithosphere*, eds Cermak, V. & Rybach, L., Springer-Verlag, Heidelberg, in press.

Savage, J. E. G. & Long, R. E., 1985. Lithospheric structure beneath the Kenya dome, *Geophys. J. R. astr. Soc.*, **83**, 461–477.

Shudofsky, G. N., 1985. Source mechanisms and focal depths of east African earthquakes using Rayleigh-wave inversion and body-wave modelling, *Geophy. J. R. astr. Soc.*, **83**, 563–614.

Shudofsky, G. N., Cloetingh, S., Stein, S. & Wortel, R., 1987. Unusually deep earthquakes in East Africa: constraints on the thermo-mechanical structure of a continental rift system, *Geophys. Res. Lett.*, **14**, 741–744.

Sibson, R. H., 1974. Frictional constraints on thrust, wrench, and normal faults, *Nature*, **249**, 542–544.

Sibson, R. H., 1982. Fault zone models, heat flow, and the depth distribution of earthquakes in the continental crust of the United States, *Bull. seism. Soc. Am.*, **72**, 151–163.

Smith, R. B. & Bruhn, R. L., 1984. Intraplate extensional tectonics of the eastern Basin-Range: inferences on structural style from seismic reflection data, regional tectonics, and thermal-mechanical models of brittle–ductile deformation, *J. geophys. Res.*, **89**, 5733–5762.

Steckler, M. S. & Ten Brink, U. S., 1986. Lithospheric strength variations as a control on new plate boundaries: examples from the northern Red Sea region, *Earth planet. Sci. Lett.*, **79**, 120–132.

Vink, G. E., Morgan, W. J. & Zhao, W.-L., 1984. Preferential rifting of continents: a source of displaced terranes, *J. geophys. Res.*, **89**, 10 072–10 076.

Von Herzen, R. P. & Vacquier, V., 1967. Terrestrial heat flow in Lake Malawi, Africa, *J. geophys. Res.*, **72**, 4221–4226.

Von Herzen, R. P., Finckh, P. & Hsu, K. J., 1974. Heat flow measurements in Swiss lakes, *J. Geophys.*, **40**, 141–172.

Williamson, K. H., 1975. Terrestrial heat flow studies in Kenya, *PhD thesis*, University of London.